JOURNAL OF MATERIALS SCIENCE 19 (1984) 125–134

# The elastic stiffness constants and their hydrostatic pressure derivatives for TGS

A. DUNK, G. A. SAUNDERS
*School of Physics, University of Bath, Claverton Down, Bath, UK*

The thirteen adiabatic elastic stiffness moduli of triglycine sulphate (TGS) have been determined at room temperature from measurements of the ultrasound wave velocities. Results are used to describe the elastic behaviour of TGS. Accidental pure mode directions have been found at 9.4° and 106.5°. A method has been developed for obtaining the hydrostatic pressure derivatives ($\partial C_{IJ}/\partial P$) of the elastic constants of a monoclinic crystal from the hydrostatic pressure dependences of ultrasound wave velocities. This method has been applied to find the $\partial C_{IJ}/\partial P$ for TGS. There is no evidence for acoustic phonon mode softening under pressure.

## 1. Introduction

The second-order elastic stiffness constants of a crystal determine the slopes of the acoustic phonon dispersion curves in the long wavelength limit; their hydrostatic pressure dependences provide information on the shift of the mode energies with compression. Experimentally the elastic constants can be obtained using standard pulsed ultrasonic techniques, while their pressure derivatives can be found from the pressure-induced changes in the ultrasonic wave velocities. For a monoclinic crystal, which is characterized by 13 independent elastic constants, extraction of the elastic constants and their pressure derivatives from ultrasonic data is fairly complex. However, procedures which can be used to obtain the elastic constants have been provided by several workers [1–3]. A method for finding their pressure derivatives is given here and is used to find them for triglycine sulphate (TGS) $(NH_2CH_2COOH)_3H_2SO_4$. At room temperature TGS is a ferroelectric crystal belonging to the monoclinic system and space group $P2_1$. The polar axis is the two-fold *b*-axis. At 49° C TGS undergoes a second-order phase transition into a paraelectric, non-piezoelectric phase. The elastic constants have been measured in both the ferroelectric [4–6] and paraelectric [7] phases. There are piezoelectric contributions to the elastic stiffness in the ferroelectric phase. These have been considered in part in a Brillouin scattering determination of the elastic constants [5] but not in the ultrasonic measurements of Konstantinova *et al.* [4]. Haussühl and Albers [7] have found that calculations of the piezoelectric corrections are unsatisfactory and suggest a requirement for high precision determinations of the piezoelectric and dielectric constants for TGS under accurately defined dielectric conditions. In view of this, they have restricted their work to a determination of the elastic constants in the paraelectric phase. The Brillouin scattering measurements of Luspin and Hauret [5], which include measurements of $C_{11}^{E}$, $C_{22}^{D}$ and $C_{33}^{E}$ in both phases suggest that the piezoelectric contributions in ferroelectric TGS are not large. Hence in this first measurement of the pressure derivatives of the elastic constants they have not been taken into account.

## 2. Determination of the elastic constants of TGS

The single crystals studied were of the highest optical quality grown for use by Dr G. R. Jones as the sensing element in the pyroelectric vidicon tube. A right-handed orthogonal axial set (0*x*, 0*y*, 0*z*) has been chosen with 0*y* parallel to the two-fold *b*-axis. The TGS crystals were orientated by first identifying the two-fold axis using the X-ray back-reflection Laue technique, then finding the *a*- and *c*-axes by reference to the crystal morphology [4]. Four cubes were cut with a diamond

0022–2461/84 $03.00 + .12  

wheel, one with faces perpendicular to the [001], [010] and [100] directions and the other three such that they had a pair of faces perpendicular to the [101], [011] and [110] directions, respectively. Faces were polished flat and parallel on a cast-iron plate first with aloxite and water for a few seconds and finished with 14 $\mu$m diamond paste. Ultrasonic waves (carrier frequency 10 MHz) were inserted and detected by quartz transducers bonded with Dow Resin 279-V9 and their velocities measured using the pulse echo overlap technique. A correction has been applied to the ultrasonic velocity, to account for the transducer effect which, depending upon the acoustic impedance mismatch between TGS and quartz, acts to alter the effective path length [8]. Velocities were measured for the ultrasonic modes listed in Table I, sufficient to enable determination of a complete set of elastic constants [1].

For a monoclinic crystal the 13 independent second-order elastic stiffness constants represented in Voigt notation ($ij \rightarrow m = i$, if $i = j$ and $ij \rightarrow n = 9 - i$ if $i \neq j$) and matrix form are:

$$C_{ij} = \begin{pmatrix} C_{11} & C_{12} & C_{13} & 0 & C_{15} & 0 \\ C_{12} & C_{22} & C_{23} & 0 & C_{25} & 0 \\ C_{13} & C_{23} & C_{33} & 0 & C_{35} & 0 \\ 0 & 0 & 0 & C_{44} & 0 & C_{46} \\ C_{15} & C_{25} & C_{35} & 0 & C_{55} & 0 \\ 0 & 0 & 0 & C_{46} & 0 & C_{66} \end{pmatrix} \quad (1)$$

To obtain these elastic constants and their hydrostatic pressure derivatives as best fits to experimental ultrasonic velocity measurements necessitates an extensive computational procedure based on solution of the Christoffel equation

$$[k^2\Gamma_{ij} - \rho v^2 \delta_{ij}]u_j = 0 \quad (2)$$

where $k$ is $2\pi/\lambda$ and $u_j$ are components of the particle displacement vector. The elements of the Christoffel matrix are:

$$\begin{aligned}
\Gamma_{11} &= C_{11}l_x^2 + C_{66}l_y^2 + C_{55}l_z^2 + 2C_{15}l_zl_x \\
\Gamma_{12} &= (C_{46} + C_{25})l_yl_z + (C_{12} + C_{66})l_xl_y \\
\Gamma_{13} &= C_{15}l_x^2 + C_{46}l_y^2 + C_{35}l_z^2 + (C_{13} + C_{55})l_zl_x \\
\Gamma_{22} &= C_{66}l_x^2 + C_{22}l_y^2 + C_{44}l_z^2 + 2C_{46}l_zl_x \quad (3) \\
\Gamma_{23} &= (C_{44} + C_{23})l_yl_z + (C_{25} + C_{46})l_xl_y \\
\Gamma_{33} &= C_{55}l_x^2 + C_{44}l_y^2 + C_{33}l_z^2 + 2C_{35}l_zl_x.
\end{aligned}$$

Here $l_x$, $l_y$, $l_z$ refer to the direction of wave propagation. The condition for non-zero solutions of the Christoffel equation is

$$\det\left[\Gamma_{ij} - \rho\frac{v^2}{k^2}\delta_{ij}\right] = 0 \quad (4)$$

which gives the mode velocity; the particle displacement vectors can be obtained by substituting the velocity into Equation 2. The relationships [3] between the elastic constants and mode velocity for selected modes are given in Table I. From measurements of the ultrasonic velocities in the six directions [001], [010], [100], [101], [110] and [011] it is possible to obtain the complete set of 13 elastic constants [1]. The appropriate solutions to the Christoffel equations are given in Tables I and II. Cross checks on the accuracy of the velocity measurements can be made using trace identities [2], which can be obtained by manipulation of the relationships in Tables I and II,

$$\rho v_4^2 + \rho v_6^2 = \rho v_2^2 + \rho v_8^2 \quad (5)$$

$1.649 \times 10^{10}\,\mathrm{N\,m^{-2}}$ $\quad$ $1.648 \times 10^{10}\,\mathrm{N\,m^{-2}}$

$$\rho v_2^2 + \tfrac{1}{2}(\rho v_1^2 + \rho v_3^2 + \rho v_5^2 + \rho v_8^2) = \rho(v_{13}^2 + v_{14}^2 + v_{15}^2) \quad (6)$$

$5.542 \times 10^{10}\,\mathrm{N\,m^{-2}}$ $\quad$ $5.527 \times 10^{10}\,\mathrm{N\,m^{-2}}$

$$\rho v_8^2 + \tfrac{1}{2}(\rho v_2^2 + \rho v_5^2 + \rho v_7^2 + \rho v_9^2) = \rho(v_{16}^2 + v_{17}^2 + v_{18}^2) \quad (7)$$

$4.923 \times 10^{10}\,\mathrm{N\,m^{-2}}$ $\quad$ $4.867 \times 10^{10}\,\mathrm{N\,m^{-2}}$

$$\rho v_2^2 \rho v_8^2 - [\rho v_{11}^2 - \tfrac{1}{2}(\rho v_2^2 + \rho v_8^2)]^2 = \rho v_4^2 \rho v_6^2 \quad (8)$$

$0.629 \times 10^{20}(\mathrm{N\,m^{-2}})^2$ $\quad$ $0.643 \times 10^{20}(\mathrm{N\,m^{-2}})^2$.

The extent to which these checks are verified attests to the internal consistency of the data.

Determination of the elastic constants from the velocity data begins with $C_{22}$, $C_{44}$ and $C_{66}$ which can be obtained directly from $v_5$, $v_8$ and $v_2$, respectively (Table I). Then $C_{46}$ can be found using $v_{11}$. Five more elastic constants are available from the relationships which follow from those in Tables I and II:

$$C_{11} + C_{55} = \rho v_1^2 + \rho v_3^2 = A \quad (9)$$

$$C_{11}C_{55} - C_{15}^2 = \rho v_1^2 \rho v_3^2 = B \quad (10)$$

$$C_{55} + C_{33} = \rho v_7^2 + \rho v_9^2 = D \quad (11)$$

$$C_{55}C_{33} - C_{35}^2 = \rho v_7^2 \rho v_9^2 = F \quad (12)$$

TABLE I Ultrasonic wave velocity and elastic constant relationships for monoclinic crystals and the pressure derivatives of the normalized overlap frequency and mode velocities for TGS. The density of TGS at 293 K is 1680 kg m$^{-3}$

| Mode symbol | Direction of wave propagation | Polarization vector | Relationship between elastic constant and wave velocity | Measured wave velocity (m s$^{-1}$) | $f'/f_0 \times 10^{-3}$ bar$^{-1}$ * | $\left(\frac{\partial \rho v^2}{\partial P}\right)_{P=0}$ |
|---|---|---|---|---|---|---|
| $v_1$ | [100] | [100] | $\rho v_1^2 = \{C_{11} + C_{55} + [(C_{11} - C_{55})^2 + 4C_{15}^2]^{1/2}\}/2$ | 5130 | 9.50 | 9.51 |
| $v_2$ | [100] | [010] | $\rho v_2^2 = C_{66}$ | 1900 | 3.50 | 0.58 |
| $v_3$ | [100] | [001] | $\rho v_3^2 = \{C_{11} + C_{55} - [(C_{11} - C_{55})^2 + 4C_{15}^2]^{1/2}\}/2$ | 2520 | 4.28 | 1.18 |
| $v_4$ | [010] | [100] | $\rho v_4^2 = \{C_{44} + C_{66} + [(C_{44} - C_{66})^2 + 4C_{46}^2]^{1/2}\}/2$ | 2460 | 3.93 | 1.01 |
| $v_5$ | [010] | [010] | $\rho v_5^2 = C_{22}$ | 4460 | 19.0 | 13.4 |
| $v_6$ | [010] | [001] | $\rho v_6^2 = \{C_{44} + C_{66} - [(C_{44} - C_{66})^2 + 4C_{46}^2]^{1/2}\}/2$ | 1940 | 3.78 | 0.61 |
| $v_7$ | [001] | [100] | $\rho v_7^2 = \{C_{33} + C_{55} - [(C_{33} - C_{55})^2 + 4C_{35}^2]^{1/2}\}/2$ | 2510 | 6.49 | 1.35 |
| $v_8$ | [001] | [010] | $\rho v_8^2 = C_{44}$ | 2490 | 4.55 | 0.92 |
| $v_9$ | [001] | [001] | $\rho v_9^2 = \{C_{33} + C_{55} + [(C_{33} - C_{55})^2 + 4C_{35}^2]^{1/2}\}/2$ | 4050 | 10.6 | 5.78 |
| $v_{10}$ | [101] | [$\bar{1}$01] | $\rho v_{10}^2 = \{(C_{11} + C_{33} + 2(C_{15} + C_{35} + C_{55}) - [4(2C_{35} + C_{33} - C_{11} - 2C_{15})^2 + (C_{15} + C_{35} + C_{13} + C_{55})^2]^{1/2}\}/4$ | 2270 | 5.15 | 0.92 |
| $v_{11}$ | [101] | [010] | $\rho v_{11}^2 = \frac{1}{2}(C_{66} + C_{44} + 2C_{46})$ | 2280 | 4.51 | 0.821 |
| $v_{12}$ | [101] | [101] | $\rho v_{12}^2 = \{(C_{11} + C_{33} + 2(C_{15} + C_{35} + C_{55}) + [4(2C_{35} + C_{33} - C_{11} - 2C_{15})^2 + (C_{15} + C_{35} + C_{13} + C_{55})^2]^{1/2}\}/4$ | 4530 | 11.4 | 8.01 |
| $v_{13}$ | [110] | [110] | $v_{13}$ to $v_{18}$ obtained as a root of third-order | 4560 | 12.8 | 9.73 |
| $v_{14}$ | [110] | [001] | algebraic equations including known | 2460 | 4.41 | 1.13 |
| $v_{15}$ | [110] | [1$\bar{1}$0] | stiffness constants. The resulting equations | 2460 | 7.99 | 1.86 |
| $v_{16}$ | [011] | [011] | are extensive. | 4550 | 12.8 | 9.26 |
| $v_{17}$ | [011] | [0$\bar{1}$1] | | 1840 | 7.41 | 0.896 |
| $v_{18}$ | [011] | [100] | | 2210 | 5.62 | 0.999 |

*1 bar $\equiv 10^5$ N m$^{-2}$.

TABLE II Additional relationships used to obtain the elastic stiffness constants

| | |
|---|---|
| | $\rho v_1^2 + \rho v_3^2 = C_{11} + C_{55}$ |
| | $\rho v_1^2 \rho v_3^2 = C_{11}C_{55} - C_{15}^2$ |
| | $\rho v_4^2 + \rho v_6^2 = C_{44} + C_{66}$ |
| | $\rho v_4^2 \rho v_6^2 = C_{66}C_{44} - C_{46}^2$ |
| | $\rho v_7^2 + \rho v_9^2 = C_{55} + C_{33}$ |
| | $\rho v_7^2 \rho v_9^2 = C_{55}C_{33} - C_{35}^2$ |
| | $\rho v_{10}^2 + \rho v_{12}^2 = \frac{1}{2}[C_{11} + C_{33} + 2(C_{15} + C_{35} + C_{55})]$ |
| | $\rho v_{10}^2 \rho v_{12}^2 = \frac{1}{4}[(C_{11} + C_{55} + 2C_{15})(C_{55} + C_{33} + 2C_{35}) - (C_{15} + C_{35} + C_{13} + C_{55})^2]$ |
| [1 1 0] direction | $4\rho^2(v_{13}^2 v_{14}^2 + v_{13}^2 v_{15}^2 + v_{14}^2 v_{15}^2) = (C_{66} + C_{22})(C_{55} + C_{44}) + (C_{11} + C_{66})(C_{66} + C_{22} + C_{55} + C_{44}) - (C_{15} + C_{46})^2 - (C_{12} + C_{66})^2 - (C_{25} + C_{46})^2$ |
| | $\rho^3 v_{13}^2 v_{14}^2 v_{15}^2 = \frac{1}{8}[(C_{11} + C_{66})(C_{66} + C_{22})(C_{55} + C_{44}) + 2(C_{15} + C_{46})(C_{25} + C_{46})(C_{12} + C_{66}) - (C_{11} + C_{66})(C_{25} + C_{46})^2 - (C_{55} + C_{44})(C_{12} + C_{66})^2 - (C_{15} + C_{46})^2(C_{66} + C_{22})]$ |
| | $\rho(v_{13}^2 + v_{14}^2 + v_{15}^2) = C_{66} + \frac{1}{2}(C_{11} + C_{22} + C_{55} + C_{44})$ |
| [0 1 1] direction | $4\rho^2(v_{16}^2 v_{17}^2 + v_{16}^2 v_{18}^2 + v_{17}^2 v_{18}^2) = (C_{22} + 2C_{44} + C_{33})(C_{66} + C_{55}) + (C_{22} + C_{44})(C_{44} + C_{33}) - (C_{46} + C_{35})^2 - (C_{46} + C_{25})^2 - (C_{44} + C_{23})^2$ |
| | $\rho^3 v_{16}^2 v_{17}^2 v_{18}^2 = \frac{1}{8}[(C_{66} + C_{55})(C_{22} + C_{44})(C_{44} + C_{33}) + 2(C_{46} + C_{35})(C_{44} + C_{23})(C_{46} + C_{25}) - (C_{66} + C_{55})(C_{44} + C_{23})^2 - (C_{46} + C_{25})^2(C_{44} + C_{33}) - (C_{22} + C_{44})(C_{46} + C_{35})^2]$ |
| | $\rho(v_{16}^2 + v_{17}^2 + v_{18}^2) = C_{44} + \frac{1}{2}(C_{66} + C_{55} + C_{22} + C_{33})$ |

$$C_{15} + C_{35} = \rho(v_{10}^2 + v_{12}^2 - \tfrac{1}{2}(v_1^2 + v_3^2 + v_7^2 + v_9^2)) = E. \quad (13)$$

Determination of the complete set of elastic constants requires considerable algebraic and numerical manipulation of the expressions in Tables I and II together with recourse to physical principles involved in the propagation of ultrasonic waves in crystals. This detail need not be reported here. The resulting adiabatic elastic stiffness constants of TGS are compared with those obtained by other workers in Table III and the compliances in Table IV. In view of the accumulation of errors involved in the extraction of the elastic constants, especially in $C_{25}$, $C_{23}$ and $C_{12}$, the agreement between the sets of data is more than reasonable.

Using the elastic stiffness constant set obtained in this work (Table II), the three wave velocities have been calculated for propagation directions at 1° intervals around the *yz*, *xz* and *xy* planes by computation of the eigenvalues of the Christoffel equations [2]. The resultant cross-sections of the three elastic wave velocity surfaces, presented in Fig. 1, follow the crystal Laue symmetry.

In general, in a crystal three distinct, mutually orthogonal elastic plane waves propagate along a given direction, these modes being neither longitudinal nor transverse. However, along certain special directions, the pure mode directions (or acoustic axes), a pure longitudinal and two pure transverse waves do propagate. Knowledge of these directions can be useful because it is usually easier to excite such modes with *X*- or *Y*-cut transducers and also there is no deviation of the energy flux from the propagation direction – minimizing the possibility of sidewall reflections. The conditions for a pure mode direction [9] are

$$\epsilon_{ijk} C_{jlrs} N_k N_l N_r N_s = 0. \quad (14)$$

TABLE III The elastic stiffness constants of TGS in the orthogonal axial set of [4]. The designations *D* (constant displacement) and *E* (constant electric field) are those given and discussed by Luspin and Hauret [5]. The units are $10^{10}\,\mathrm{N\,m^{-2}}$

| $C_{11}^E$ | $C_{22}^D$ | $C_{33}^E$ | $C_{44}^D$ | $C_{55}^E$ | $C_{66}^D$ | $C_{12}^D$ | $C_{13}^E$ | $C_{23}^D$ | $C_{15}^E$ | $C_{25}^D$ | $C_{35}^E$ | $C_{46}^D$ | Ref. |
|---|---|---|---|---|---|---|---|---|---|---|---|---|---|
| 4.55 | 3.21 | 2.63 | 0.95 | 1.11 | 0.62 | 1.72 | 1.98 | 2.08 | −0.30 | −0.036 | −0.50 | −0.026 | [4] |
| 4.71 | 3.35 | 2.75 | 1.02 | 1.03 | 0.61 | 1.50 | 2.10 | 1.85 | −0.18 | −0.20 | 0.05 | −0.02 | [5] |
| 4.41 | 3.34 | 2.73 | 1.04 | 1.08 | 0.61 | 1.89 | 1.67 | 1.97 | −0.21 | −0.19 | −0.18 | 0.05 | This work |
| 4.61 | – | 2.79 | – | 1.12 | – | – | 2.10 | – | −0.22 | – | 0.15 | – | [6] |

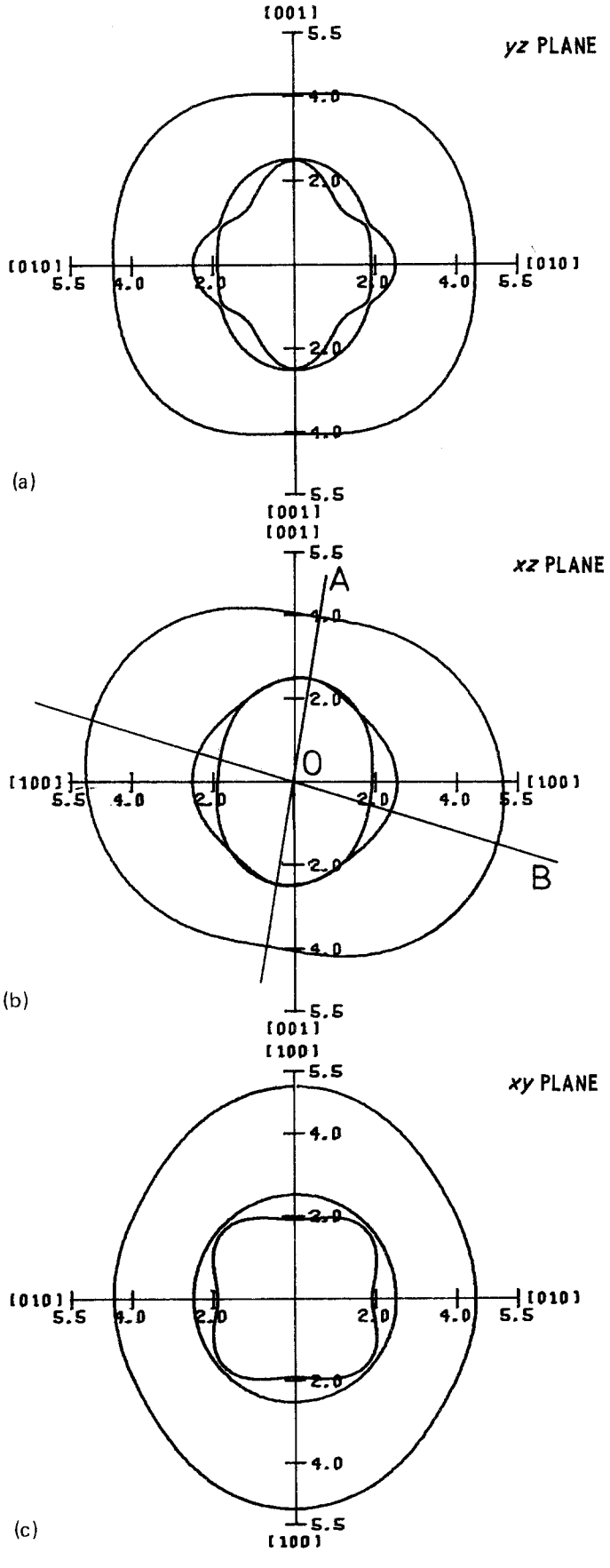


*Figure 1* *yz*, *xz* and *xy* plane cross-sections of elastic wave velocity surfaces of TGS at 293 K. Units are $10^3 m s^{-1}$, the scales being the same for the abscissae and ordinates of each diagram. The outside curve in each case corresponds to the quasi-longitudinal modes, which have the highest velocity. The lines OA and OB in the *xz* plane denote the accidental pure mode direction at 9.4° and 106.5°, respectively, from the $+z$-axis towards the $+x$-axis.

TABLE IV The elastic compliances of TGS. Units are $10^{-11}\,m^2\,N$

| $S_{11}$ | $S_{22}$ | $S_{33}$ | $S_{44}$ | $S_{55}$ | $S_{66}$ | $S_{12}$ | $S_{13}$ | $S_{23}$ | $S_{15}$ | $S_{25}$ | $S_{35}$ | $S_{46}$ | Ref. |
|---|---|---|---|---|---|---|---|---|---|---|---|---|---|
| 3.29 | 6.98 | 10.85 | 10.53 | 10.73 | 16.15 | −0.29 | −2.27 | −5.77 | −0.14 | −2.45 | 4.08 | 0.44 | [4] |
| 3.27 | 4.87 | 7.74 | 9.81 | 10.11 | 16.40 | −0.06 | −2.47 | −3.25 | 0.68 | 1.09 | −1.44 | 0.32 | [5] |
| 3.19 | 5.62 | 6.79 | 9.65 | 9.39 | 16.45 | −1.13 | −1.12 | −3.35 | 0.23 | 0.21 | 0.32 | −0.79 | This work |

For a monoclinic crystal solution in the $xz$ plane can can be shown to be

$$N_1N_3[N_1^2A_1 - N_3^2C_1] + N_1^2(3N_3^2 - N_1^2)C_{15} - N_3^2(3N_1^2 - N_3^2)C_{35} = 0, \quad (15)$$

or writing the direction cosine ratio $N_1/N_3$ as $u$

$$-u^4C_{15} + A_1u^3 + 3u^2(C_{15} - C_{35}) - u_1C_1 + C_{35} = 0. \quad (16)$$

Here $A_1 = C_{11} - 2C_{55} - C_{13}$ and $C_1 = C_{33} - 2C_{55} - C_{13}$. Substituting the elastic constant values obtained from this work (Table I) into this equation, shows that there is a pure mode axis for TGS in the $xz$ plane at 9.4° from the $+z$ axis towards the $+x$ axis; this position is shown in Fig. 1. A second pure mode axis occurs at 106.5°.

Knowledge of the elastic stiffness tensor components enables determination of a material's response to any applied stress within the Hooke's law regime. Young's modulus $E$, the measure of the ratio of an applied longitudinal stress to the resulting longitudinal strain, for a monoclinic crystal [10] is

$$E = \{l_1^4S_{11} + 2l_1^2l_2^2S_{12} + 2l_1^2l_3^2S_{13} + 2l_1^3l_3S_{15} + l_2^4S_{22} + 2l_2^2l_3^3S_{23} + 2l_1l_2^2l_3S_{25} + l_3^4S_{33} + 2l_1l_3^3S_{35} + l_2^2l_3^2S_{44} + 2l_1l_2^2l_3S_{46} + l_1^2l_3^2S_{55} + l_1^2l_2^2S_{66}\}^{-1} \quad (17)$$

for a stress in the direction labelled by the direction cosines $l_1$, $l_2$, $l_3$. Young's modulus can be represented by a surface which gives a useful visual guide to the elastic behaviour of a crystal. Three plane ($yz$, $xz$ and $xy$) cross-sections of this surface for TGS are presented in Fig. 2. For a given stress applied along a crystallographic axis, the strain is greatest along the $z$-axis and least along the $x$-axis.

The volume compressibility $-\Delta/P$ (where $\Delta$ is the dilation) is $S_{iikk}$ (or in Voigt notation $S_{11} + S_{22} + S_{33} + 2(S_{12} + S_{23} + S_{31})$) equal to $4.4 \times 10^{-11}\,m^2\,N$ for TGS. Hence the bulk modulus, defined as the reciprocal of the compressibility is $2.27 \times 10^{11}\,N\,m^{-2}$. Another elastic property commonly required is the linear compressibility, which is the relative decrease in length of a line when a crystal is subjected to hydrostatic pressure and is given by $S_{ijkk}l_il_j$. Here $l_i$ is a unit vector in the direction of the stretch of the line. For a monoclinic crystal the linear compressibility is [10]

$$\beta = (S_{11} + S_{12} + S_{13})l_1^2 + (S_{12} + S_{22} + S_{23})l_2^2 + (S_{13} + S_{23} + S_{33})l_3^2 + (S_{15} + S_{25} + S_{35})l_3l_1. \quad (18)$$

The marked anisotropic behaviour of the linear compressibility of TGS can be seen in the $yz$, $xz$ and $xy$ plane plots of the property in Fig. 3.

There is a simplifying feature of the elastic behaviour of TGS which is a helpful guide and may well be of practical value. This can be seen by considering Matrix 1 which collates the elastic constants. Now the elastic constants $C_{15}$, $C_{25}$, $C_{35}$ and $C_{46}$ are an order of magnitude smaller than the others (Table III). If they were zero, the matrix would be that for an orthorhombic crystal. The wave velocity (Fig. 1), Young's modulus (Fig. 2) and compressibility surface (Fig. 3) cross-sections, especially those of $yz$ and $xy$ planes, show clearly this pseudo-orthorhombic elastic behaviour of TGS. In the $xz$ plane the surfaces are rotated away from the crystallographic $x$- and $z$-axis to the acoustic axes; there is some distortion because the two acoustic axes in the $xz$ plane are not perpendicular to each other.

The unit cell volume of TGS is $0.640\,nm^3$; there are two formula units, each comprising 37 atoms, per primitive unit cell [11]. Hence there are $3N$ (= 222) degrees of freedom and therefore $3N$ phonon modes at the Brillouin zone centre. This complex vibration spectrum makes for difficulties in quantitative analysis of lattice vibration properties. Thus it is useful to have an estimate of the Debye temperature, $\theta_D$, corresponding to the acoustic modes alone, which can be obtained from the measured elastic constants by integrating

$$\theta_D = \left(\frac{9N}{4\pi V}\right)^{1/3} \frac{h}{k} \Big/ \left[\int \left(\frac{1}{v_1^3} + \frac{1}{v_2^3} + \frac{1}{v_3^3}\right) \frac{d\Omega}{\pi}\right]^{1/3}$$

over velocity space. Here the $v_i$ ($i = 1, 2, 3$) are the three velocities obtained as the eigenvalues of the

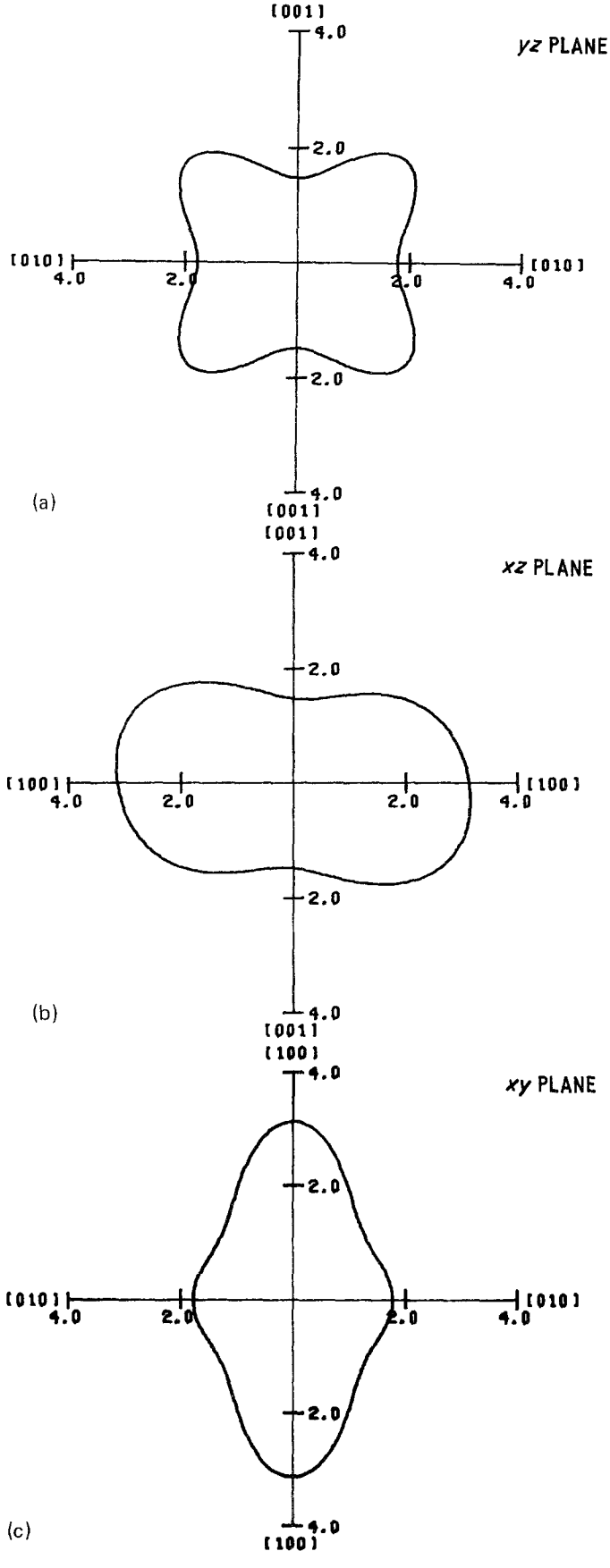


*Figure 2* *yz*, *xz* and *xy* plane cross-sections of the Young's modulus surface of TGS. Units are $10^{10}\,N\,m^{-2}$, the scales being equal for the abscissae and ordinates of each diagram.

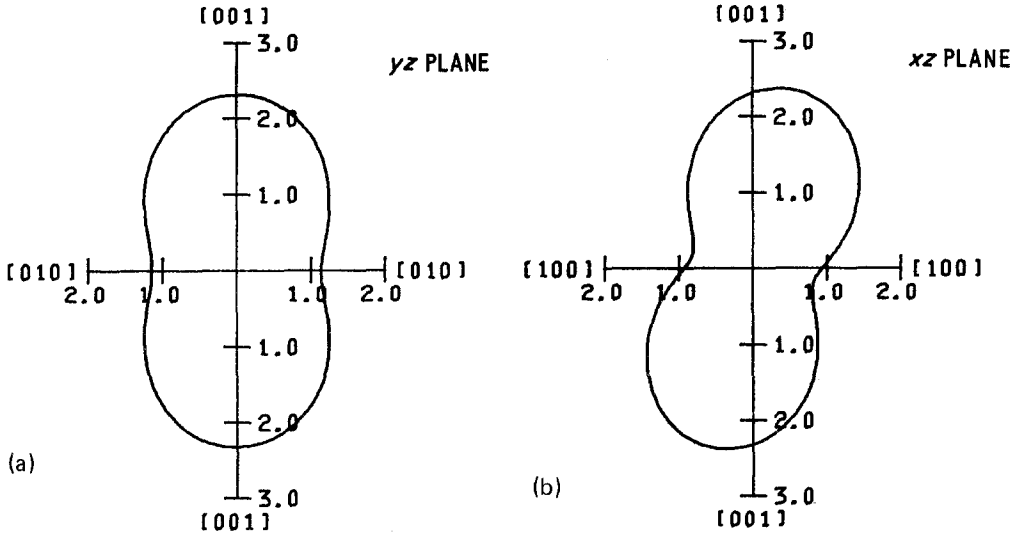


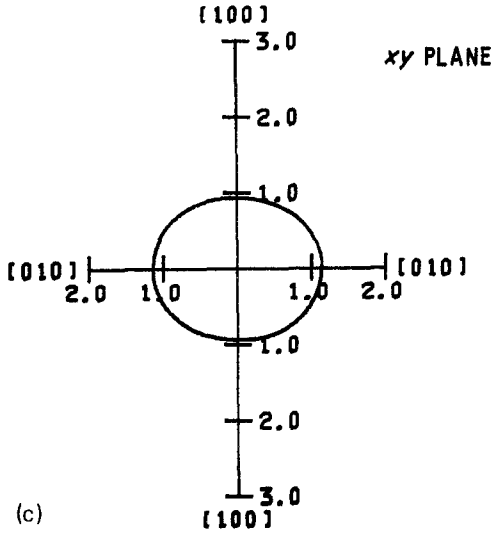


*Figure 3* $yz$, $xz$ and $xy$ plane cross-sections of the linear compressibility surface of TGS. Units are $10^{-10}\,m^2\,N^{-1}$, the scales being equal for the abscissae and ordinates of each diagram.

Christoffel Equations 2 for a given direction. This integration has been carried out over the whole of velocity space for all three modes (the curves in Fig. 1 show only the $yz$, $xz$ and $xy$ plane cross-sections of these velocity surfaces). The integral over solid angle has been approximated by a sum taken at 10 288 points each subtending an equal solid angle $\Delta\Omega$ of $1.218 \times 10^{-3}$ steradians. The Debye temperature $\theta_D$ of TGS calculated from the room temperature elastic constants (Table III) is 170 K. Using the room temperature, rather than low temperature elastic constant data, can be expected to produce quite a large error (of the order of 10 K) in $\theta_D$. Lawless [12] found that the low-temperature specific heats of several ferroelectrics, including TGS, are complex and involve, in addition to the Debye $T^3$ term, a $T^{3/2}$ component, which he ascribed to a contribution from domain walls. He obtained a value of 107 K for $\theta_D$ for TGS. Thus there is a substantial difference between the Debye temperatures obtained from the specific heat and elastic constants, perhaps not surprisingly in view of the complexities of the lattice dynamical behaviour and the domain wall effects which must be present in TGS.

## 3. A procedure for determination of the hydrostatic pressure derivatives of the elastic stiffness constants for a monoclinic crystal

The hydrostatic pressure dependences of these ultrasonic wave velocities were measured at pressures up to 2 kbar ($\equiv 2 \times 10^8$ Pa) in a piston and cylinder apparatus [13]. Pressure was determined by a manganin wire resistance gauge.

The pulse echo overlap frequency was converted to a relative change $(\Delta W/W_0 - 1)$ in the natural velocity $W$ [14]. The initial pressure derivative of $\rho v^2$ can be obtained using [15]

$$(\rho v^2)'_{P=0} = \rho v_0^2(2f'/f_0 + \chi^T - 2N_k N_m S^T_{kmii}), \tag{19}$$

where $\chi^T$ is the isothermal volume compressibility, $N_k N_m S^T_{kmii}$ corresponds to the isothermal linear compressibility, $f_0$ the frequency required for pulse overlap at atmospheric pressure and $f'$ is the associated pressure derivative. The values of $f'$,

determined as the gradient of the least square line of the frequency against pressure plot, normalized to $f_0$ are given as $f'/f_0$ in Table I. This equation in this form holds strictly only for pure mode directions, where the pressure dependence of the particle displacement vector is zero. In a monoclinic crystal this is true only for a few modes. However, if the effect of pressure on the particle displacement vector is small, Equation 19 can be taken as a reasonable approximation. Although in a determination of $(\rho v^2)'_{P=0}$ through Equation 2 the isothermal elastic constants should be used, the difference between isothermal and adiabatic elastic constants is not substantial compared with the experimental error and the adiabatic compliances have been employed here. The pressure derivatives $(\rho v^2)'_{P=0}$, taking into account changes in path length and density induced by pressure using Equation 2, measured for 18 modes are given in Table I. These results have been used to obtain a set of hydrostatic pressure derivatives of the elastic stiffness constants. While determination of the elastic constants themselves leads to several possible solution sets (the correct one has been deduced by arguments based on the physics of ultrasonic wave propagation), a single solution is obtained for the pressure derivatives.

The pressure derivatives are found by differentiation and manipulation of the expressions in Table I and II. Those of $C_{22}$, $C_{44}$ and $C_{66}$ have been obtained directly from

$$\frac{\partial C_{22}}{\partial P} = \frac{\partial(\rho v_5^2)}{\partial P}; \quad \frac{\partial C_{44}}{\partial P} = \frac{\partial(\rho v_8^2)}{\partial P}; \quad \frac{\partial C_{66}}{\partial P} = \frac{\partial(\rho v_2^2)}{\partial P}.$$

The next pressure derivative, which is easily found, is that of $C_{46}$ from

$$\frac{\partial \rho v_{11}^2}{\partial P} = \frac{1}{2}\left(\frac{\partial C_{44}}{\partial P} + \frac{\partial C_{66}}{\partial P} + 2\frac{\partial C_{46}}{\partial P}\right). \quad (20)$$

The pressure derivatives of $C_{11}$, $C_{55}$, $C_{15}$, $C_{33}$ and $C_{35}$ can be obtained by taking derivatives of Equations 9 to 13:

$$\frac{\partial \rho v_1^2}{\partial P} + \frac{\partial \rho v_3^2}{\partial P} = \frac{\partial C_{11}}{\partial P} + \frac{\partial C_{55}}{\partial P} = A' \quad (21)$$

$$\rho v_1^2 \frac{\partial \rho v_3^2}{\partial P} + \rho v_3^2 \frac{\partial \rho v_1^2}{\partial P} = C_{11}\frac{\partial C_{55}}{\partial P} + C_{55}\frac{\partial C_{11}}{\partial P} - 2C_{15}\frac{\partial C_{15}}{\partial P} = B' \quad (22)$$

$$\frac{\partial \rho v_7^2}{\partial P} + \frac{\partial \rho v_9^2}{\partial P} = \frac{\partial C_{55}}{\partial P} + \frac{\partial C_{33}}{\partial P} = C' \quad (23)$$

$$\rho v_7^2 \frac{\partial \rho v_9^2}{\partial P} + \rho v_9^2 \frac{\partial \rho v_7^2}{\partial P} = C_{33}\frac{\partial C_{55}}{\partial P} + C_{55}\frac{\partial C_{33}}{\partial P} - 2C_{35}\frac{\partial C_{35}}{\partial P} = D' \quad (24)$$

$$\frac{\partial}{\partial P}[\rho(v_{10}^2 + v_{12}^2 - \tfrac{1}{2}(v_1^2 + v_3^2 + v_7^2 + v_9^2)] = \frac{\partial C_{15}}{\partial P} + \frac{\partial C_{35}}{\partial P} = E'. \quad (25)$$

These equations do not contain a squared term: only one solution exists for each derivative. $C'_{55}$ can be obtained from

$$\frac{\partial C_{55}}{\partial P} = \frac{2E'C_{15}C_{35} + B'C_{35} + D'C_{15} - C_{35}C_{55}A' - C_{15}C_{55}C'}{(C_{35}C_{11} - C_{35}C_{55} + C_{15}C_{33} - C_{15}C_{55})}. \quad (26)$$

Then by back substitution $C'_{11}$, $C'_{33}$, $C'_{15}$ and $C'_{35}$ are determined. The starting point for $C_{13}$ is the equation for $4\rho v_{10}^2 \rho v_{12}^2$ in Table II which on differentiation by the product rule and rearranging gives:

$$C'_{13} = \tfrac{1}{2}(C_{15} + C_{35} + C_{13} + C_{55})^{-1}[(C_{55} + C_{33} + 2C_{35})\frac{\partial}{\partial P}(C_{11} + C_{55} + 2C_{15}) + (C_{11} + C_{55} + 2C_{15})\frac{\partial}{\partial P}(C_{55} + C_{33} + 2C_{35}) - 4(\rho v_{10}^2 \frac{\partial}{\partial P} v_{12}^2 + \rho v_{12}^2 \frac{\partial}{\partial P} v_{10}^2 - \frac{\partial}{\partial P}(C_{15} + C_{35} + C_{55})]. \quad (27)$$

The best method for obtaining the pressure derivatives of the remaining three stiffness constants $C_{25}$, $C_{12}$ and $C_{13}$ is to substitute the measured velocities at different pressures into the equations in Table II for the [1 1 0] and [0 1 1] modes to obtain these elastic constants as a function of pressure. Then their derivatives can be obtained. Taking derivatives directly of these equations leads to serious cumulative errors in $C'_{25}$, $C'_{12}$ and $C'_{13}$.

This provides a general procedure for determination of the hydrostatic pressure derivatives of the elastic stiffness constants for a monoclinic crystal. The results obtained for TGS are given in Table V. As a rule in a crystal, in the absence of mode softening, the phonon mode frequencies $\omega$ increase under pressure, so that $d\omega/d\mathbf{q}$ (where $\mathbf{q}$ is

TABLE V Hydrostatic pressure derivatives of the elastic stiffness constants of TGS

| | | |
|---|---|---|
| $\left(\frac{\partial C_{11}}{\partial P}\right)_{P=0} = 9.5;$ | $\left(\frac{\partial C_{12}}{\partial P}\right)_{P=0} = 8.9;$ | $\left(\frac{\partial C_{13}}{\partial P}\right)_{P=0} = 6.0;$ |
| $\left(\frac{\partial C_{15}}{\partial P}\right)_{P=0} = -0.40;$ | $\left(\frac{\partial C_{22}}{\partial P}\right)_{P=0} = 13.4;$ | $\left(\frac{\partial C_{23}}{\partial P}\right)_{P=0} = 6.9;$ |
| $\left(\frac{\partial C_{25}}{\partial P}\right)_{P=0} \approx 0;$ | $\left(\frac{\partial C_{33}}{\partial P}\right)_{P=0} = 5.9;$ | $\left(\frac{\partial C_{35}}{\partial P}\right)_{P=0} = 0.43;$ |
| $\left(\frac{\partial C_{44}}{\partial P}\right)_{P=0} = 0.92;$ | $\left(\frac{\partial C_{46}}{\partial P}\right)_{P=0} = 0.07;$ | $\left(\frac{\partial C_{55}}{\partial P}\right)_{P=0} = 1.2;$ |
| | $\left(\frac{\partial C_{66}}{\partial P}\right)_{P=0} = 0.58.$ | |

the phonon wave vector) also increases. Therefore, at the zone centre for the acoustic branches, the elastic wave velocities increase under pressure. For every acoustic mode measured for TGS the ultrasonic wave velocity increased with pressure: the behaviour is normal. Hence the pressure derivatives of the elastic stiffness constants are positive; $\partial C_{I5}/\partial P$ is an exception but in itself does not correspond to any normal mode – it is obtained only in combination with other derivatives $\partial C_{IJ}/\partial P$. This normal behaviour of the elastic modes under pressure has some important ramifications in understanding the nature of the phase transition which occurs at 49° C. Structural phase transitions are often associated with softening of acoustic or optic phonon modes. For an elastic phase transition, in which the crystal structure change takes place by a homogeneous lattice deformation, the associated soft mode is a long wavelength, zone centre acoustic phonon. This type of mode softening commonly results in an anomalous pressure-induced decrease of an ultrasonic wave velocity. Optic phonon mode softening is another widespread characteristic of structural phase transitions; if the soft mode is at the zone centre, then interaction between the softening optic branch and the acoustic branch can lead to acoustic mode softening, and again negative $\partial C_{IJ}/\partial P$ can occur. However, for TGS at room temperature, which is quite close to $T_c$, the hydrostatic pressure dependences of the elastic constants are positive: there is no sign of acoustic mode softening. This conclusion is in agreement with measurements of the elastic constants as a function of temperature up to and through $T_c$ [5, 6]: there are no large, anomalous decreases in ultrasound wave velocity in TGS as it approaches $T_c$.


## Acknowledgements

We are most grateful to G. R. Jones and E. H. Putley of the Royal Signals and Radar Establishment (Great Malvern) for supplying the crystals and for leading the pyroelectric crystal project of which this work is part. We would also like to thank J. Penfold and G. D. Pitt for allowing us to use the SERC high-pressure facilities at Standard Telecommunications Laboratories Limited, Harlow, and Mrs W. A. Lambson for assistance with sample preparation.


## References


1. K. S. ALEKSANDROV, *Sov. Phys. Cryst.* **3** (1958) 630.
2. H. B. HUNTINGTON, S. G. GRANGOLI and J. L. MILLS, *J. Chem. Phys.* **50** (1969) 3844.
3. K. HIROSHI, Y. ISHABASHI and Y. TAKAGI, *J. Phys. Soc. Jpn.* **35** (1973) 1450.
4. V. P. KONSTANTINOVA, I. M. SILVESTROVA and K. S. ALEKSANDROV, *Sov. Phys. Cryst.* **4** (1960) 63.
5. Y. LUSPIN and G. HAURET, *Ferroelectrics* **15** (1977) 43.
6. Z. TYLCZYŃSKI, *Physica* **111B** (1981) 267.
7. S. HAUSSÜHL and J. ALBERS, *Ferroelectrics* **15** (1977) 73.
8. E. KITTINGER, *Ultrasonics* **15** (1977) 30.
9. K. BRUGGER, *J. Appl. Phys.* **36** (1965) 759.
10. J. NYE, "Physical Properties of Crystals" (Clarendon Press, Oxford, 1957).
11. E. A. WOOD and A. N. HOLDEN, *Acta Crystallogr.* **10** (1957) 145.
12. W. N. LAWLESS, *Phys. Rev. Lett.* **36** (1976) 478.
13. Y. K. YOGURTÇU, A. J. MILLER and G. A. SAUNDERS, *J. Phys. C: Solid State Phys.* **13** (1980) 685.
14. R. N. THURSTON and K. BRUGGER, *Phys. Rev.* **133** (1964) A1604.
15. R. N. THURSTON, *Proc. IEEE* **53** (1965) 1320.



*Received 20 April*
*and accepted 26 April 1983*